Supplementary Information (SI) for Journal of Materials Chemistry A.

Mono-methyl viologen: A promising anolyte for alkaline aqueous redox flow batteries

Devendra Y. Nikumbe[a,d], R. Govindha Pandi[c], Anusuya Saha[b,d], Bhavana Bhatt[a], Surjit Bhai[b,d], Bishwajit Ganguly[b,d], Shanmugam Senthil Kumar[c] and Rajaram K. Nagarale[a,d]

[a.] *Electro Membrane Processes Laboratory, Membrane Science and Separation Technology Division, CSIR-Central Salt and Marine Chemicals Research Institute, Bhavnagar 364002, India*

[b.] *Analytical And Environmental Science Division And Centralized Instrument Facility CSIR-Central Salt and Marine Chemicals Research Institute, Bhavnagar 364002, India*

[c.] *Electrodics and Electro Catalysis Division, CSIR - Central Electrochemical Research Institute (CECRI), Karaikudi, - 630 003, India*

[d.] *Academy of Scientific and Innovative Research (AcSIR), Ghaziabad 201002, India**Experimental Details*

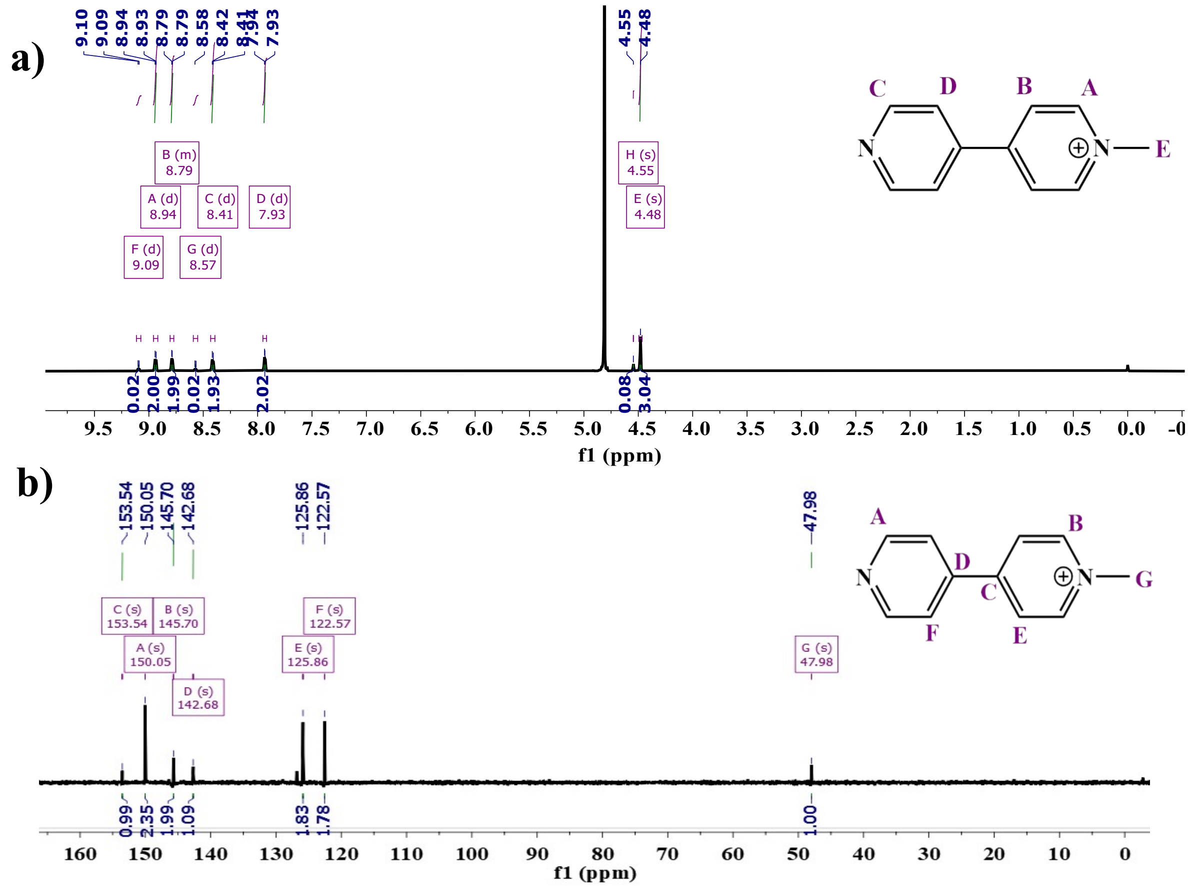

Fig. S1. (a) ^{1}H NMR of synthetic MMV, and (b) ^{13}C NMR of synthetic MMV a)

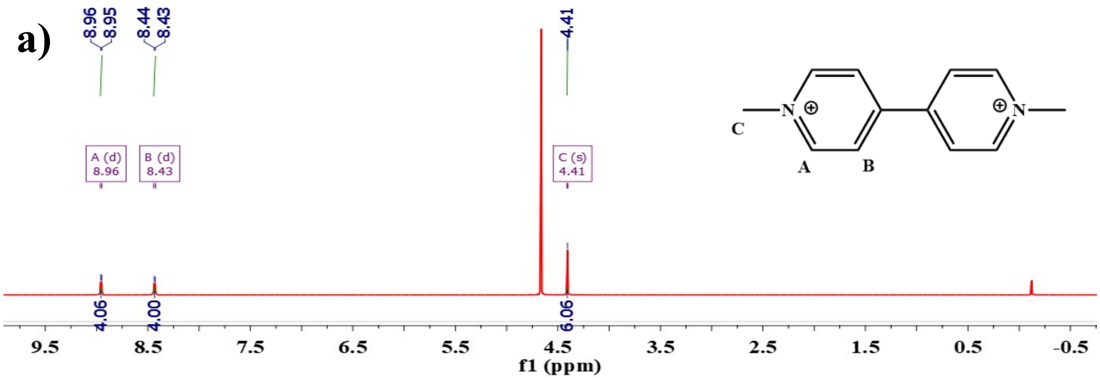

b)

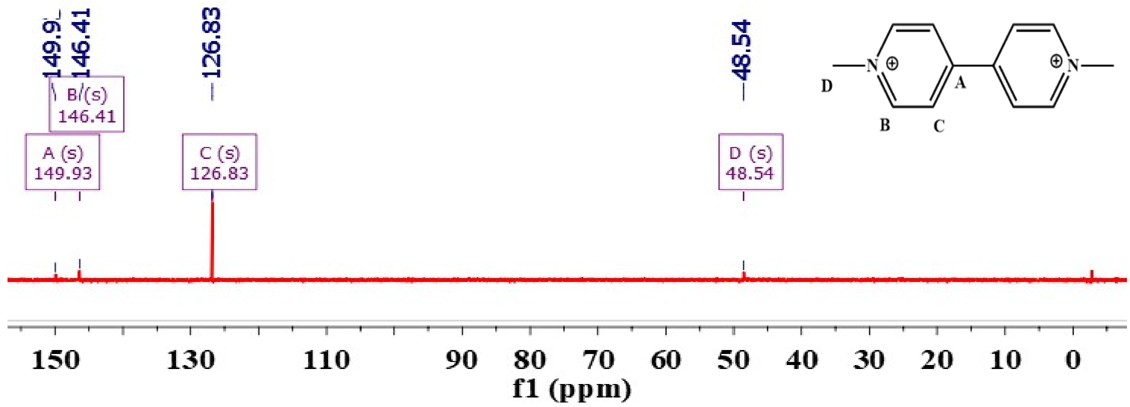

Fig. S2 (a) ^{1}H NMR of synthetic DMV, (b) ^{13}C NMR of synthetic DMV

Table S1. Properties of Interpolymer anion exchange membrane (IPAEM)[1].

Membrane	**Structure properties**	**Ion-exchange capacity (meq/g)**	**Thickness (mm)**	**Water content (%)**	**Area resistance (Ω cm²)**	**Permselectivity (%)**
IPAEM	Anion LDPE/HDPE	0.8–0.9	0.16–0.18	15	2.0–4.0	92

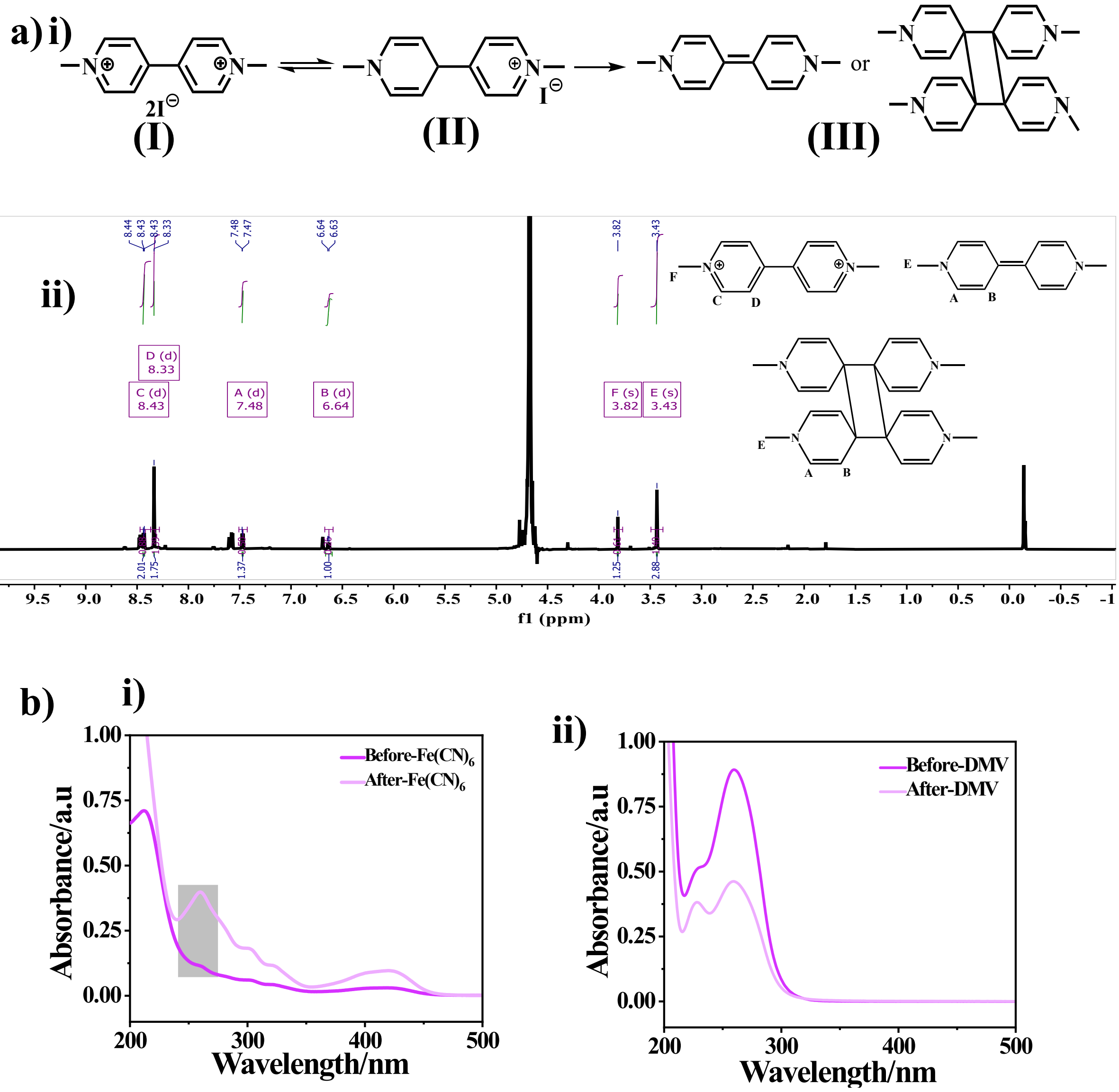

Fig. S3 Parameter leading to capacity loss (a) (i) Side reaction of DMV as well as dimer formation (ii) confirmation of side product by ^{1}H NMR. (b) UV-spectra of crossover electrolyte

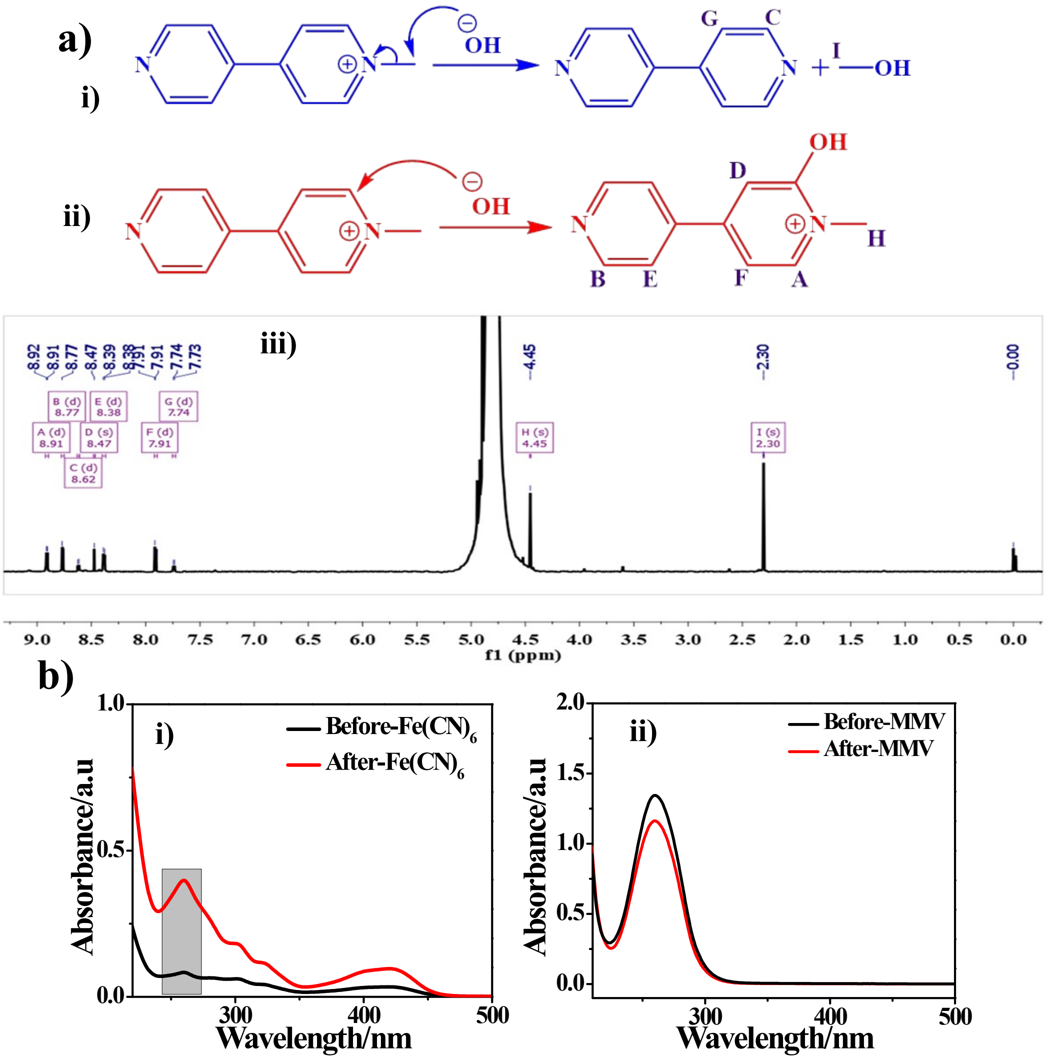

Fig. S4 Parameter leading to capacity loss (a) Side reactions of viologen (i) SN^2 reaction, (ii) nucleophilic aromatic substitution reaction, (iii) confirmation of side product i and ii by ^1H NMR. (b) UV-spectra of crossover electrolyte

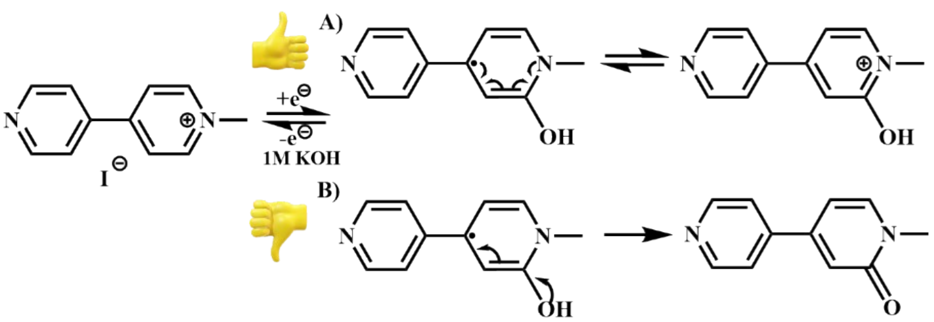

Fig. S5 degradation of mechanism of MMV in aqueous alkaline medium

Table S2. Comparison chart of All ORFBs.

Negolyte/ posolyte	Solubility in water	Concentration	Current Density, CE, EE	Capacity retention	Cell cycle number	Peak power density	Ref.
AQDS/SBQ	2 M	1 M H_2SO_4	98%, NA	99.95% per cycle	25	-	2
2,6-DHAQ /$Fe(CN)_6^{4-}$	1 M	1 M KOH	100 mA cm^{-2} 99%, 84%	99.9% per cycle	100	450 mW cm^{-2}	3
DHBQ/$K_4Fe(CN)_6$	> 8 M in 1 M KOH	1 M KOH	100 mA cm^{-2} 99%, 65%	99.76% per cycle	150	300, 164, and 137 mW cm^{-2}	4
Alloxazine/ $K_4Fe(CN)_6$ + $K_3Fe(CN)_6$	1 M	1 M KOH	100 mA cm^{-2} 99.7%,	99.98% per cycle	400	350 mW cm^{-2}	5
FMN-Na/ $K4Fe(CN)_6$	1 M	1 M KOH and 1.5 M with nicotinamide additive Average	100 mA cm^{-2} 99%	99%	200	160 mW cm^{-2}	6
4-hydroxy TEMPO/ MVi_2	2.1 M	1.5 M NaCl	40 mA cm^{-2} 99%, 70.9%	99%	100	NA	7
4-sulfate-TEMP/ Zn	1 M	1 M in 2 M $ZnCl_2$ + 2 M NH_4Cl	40 mA cm^{-2} 98.1%, 65%	93.6%	1100	NA	8
MV/ FcNCl	3.5 M	1 M NH_4Cl	60 mA cm^{-2} > 99%, 65%	81%,	500	100 $mWcm^{-2}$	9
$BTMAP_2$+-Vi2+/ $BTMAP_2$+-Fc	2.0 M	1 M NaCl	50 mA cm^{-2} > 99.95%, > 65%	98.58%,	250	NA	10
(SPr) $_2$V/KI	2.0 M	2 M KCl	60 mA cm^{-2} > 99%, 58%	94.1%,	300	67.5 mW cm^{-2}	11
BSP-Vi/ DS-Fc	2.0 M	0.5 M $NaNO_3$	96%	90%	70	NA	12
DMV/ $K_4Fe(CN)_6$ + $K_3Fe(CN)_6$	**3.5 M**	**0.5 M in 1 M NH_4Cl**	**80 mA cm^{-2} 98%, 57%**	**98.9% Per cycle**	**200**	**76 mW cm^{-2}**	**This work**
MMV/ $K_4Fe(CN)_6$ + $K_3Fe(CN)_6$	**2.5 M**	**0.8 M in 1 M KOH**	**100 mA cm^{-2} 98%, 61%**	**99.9% Per cycle**	**500**	**113 mW cm^{-2}**	**This work**

Computational Methodology

All geometries of studied isodesmic reactions were fully optimized using the B3LYP/6-311++G(d,p) level of theory in the aqueous phase using the SMD solvation model[13-15]. The confirmation of minimum optimized geometries were carried out by analysis of positive vibrational frequencies. The binding energies were calculated using Equation 4.

$$\text{Binding Energy, } (\Delta E) = E_{products} - E_{reactants} \quad (4)$$

Where $E_{products}$ refers to the sum of the energies of products and $E_{reactants}$ refers to the sum of the energies of reactants in studied isodesmic reactions, respectively. All the calculations were performed using the Gaussian 09 suite of program[16].

References

1. R. K. Nagarale, G. S. Gohil, and V. K. Shahi, Recent developments on ion-exchange membranes and electro-membrane processes, *Adv. Colloid Interface Sci.,* 119 (2006) 97-130, https://doi.org/10.1016/j.cis.2005.09.005
2. K. Wedege, E. Dražević, D. Konya, and A. Bentien. Organic Redox Species in Aqueous Flow Batteries: Redox Potentials, Chemical Stability and Solubility, Scientific RepoRts, 6:39101, DOI: 10.1038/srep39101
3. K. Lin, Q. Chen, M. R. Gerhardt, L. Tong, S. B. Kim, L. Eisenach, A. W. Valle, D. Hardee, R. G. Gordon, M. J. Aziz, and M. P. Marshak Alkaline quinone flow battery. Science 2015, 349, 1529–1532.
4. Yang, Z. J.; Tong, L. C.; Tabor, D. P.; Beh, E. S.; Goulet, M. A.; De Porcellinis, D.; Aspuru-Guzik, A.; Gordon, R. G.; Aziz, M. J. Alkaline benzoquinone aqueous flow battery for large-scale storage of electrical energy. Adv. Energy Mater. 2018, 8, 1702056.
5. K. Lin, R. Gómez-Bombarelli, U. S. Beh, L. Tong, Q. Chen, A. Valle3, A. Aspuru-Guzik, M. J. Aziz, and R. G. Gordon, A redox-flow battery with an alloxazine-based organic electrolyte. Nat Energy 2016, 1, 16102.
6. A. Orita, M. G. Verde, M. Sakai, and Y. S. Meng, A biomimetic redox flow battery based on flavin mononucleotide. Nat. Commun. 2016, 7, 13230.
7. T. Liu, X. Wei, Z. Nie, V. Sprenkle, and W. Wang, A Total Organic Aqueous Redox Flow Battery Employing a Low Cost and Sustainable Methyl Viologen Anolyte and 4-HO-TEMPO Catholyte, Adv. Energy Mater, 2016, 6, 1501449. DOI: 10.1002/aenm.201501449
8. J. Winsberg, C. Stolze, A. Schwenke, S. Muench, M. D. Hager, and U. S. Schubert, Aqueous 2,2,6,6-tetramethylpiperidine-N-oxyl catholytes for a high-capacity and high current density oxygen-insensitive hybrid-flow battery. ACS Energy Lett. 2017, 2, 411–416.

9. B. Hu, C. DeBruler, Z. Rhodes, and T. L. Liu, Long-cycling aqueous organic redox flow battery (AORFB) toward sustainable and safe energy storage. J. Am. Chem. Soc. 2017, 139, 1207–1214.
10. Beh, E. S.; De Porcellinis, D.; Gracia, R. L.; Xia, K. T.; Gordon, R. G.; Aziz, M. J. A neutral pH aqueous organic–organometallic redox flow battery with extremely high capacity retention. ACS Energy Lett. 2017, 2, 639–644.
11. C. DeBruler, B. Hu, J. Moss, J. Luo, and T. L. Liu A sulfonate-functionalized viologen enabling neutral cation exchange, aqueous organic redox flow batteries toward renewable energy storage. ACS Energy Lett. 2018, 3, 663–668.
12. J. Montero, W. da Silva Freitas, B. Mecheri, M. Forchetta, P. Galloni, S. Licoccia, and A. D'Epifanio, A Neutral-pH Aqueous Redox Flow Battery Based on Sustainable Organic Electrolytes, ChemElectroChem 2023, 10, e202201002, doi.org/10.1002/celc.202201002
13. A. D. McLean and G. S. Chandler, J. Chem. Phys., 1980, 72, 5639–5648.
14. M. J. Frisch, J. A. Pople and J. S. Binkley, J. Chem. Phys., 1984, 80, 3265–3269.
15. A. V. Marenich, C. J. Cramer and D. G. Truhlar, J. Phys. Chem. B, 2009, 113, 6378–6396.
16. M. A. R. M. J. Frisch, G. W. Trucks, H. B. Schlegel, G. E. Scuseria, H. J. R. Cheeseman, G. Scalmani, V. Barone, B. Mennucci, G. A. Petersson, J. Nakatsuji, M. Caricato, X. Li, H. P. Hratchian, A. F. Izmaylov, J. Bloino, G. Zheng, M. I. L. Sonnenberg, M. Hada, M. Ehara, K. Toyota, R. Fukuda, J. Hasegawa, J. T. Nakajima, Y. Honda, O. Kitao, H. Nakai, T. Vreven, Jr, J. A. Montgomery, V. N. E. Peralta, F. Ogliaro, M. Bearpark, J. J. Heyd, E. Brothers, K. N. Kudin, J. C. Staroverov, R. Kobayashi, J. Normand, K. Raghavachari, A. Rendell, J. E. Burant, S. S. Iyengar, J. Tomasi, M. Cossi, N. Rega, J. M. Millam, M. Klene, R. E. S. Knox, J. B. Cross, V. Bakken, C. Adamo, J. Jaramillo, R. Gomperts, R. L. M. O. Yazyev, A. J. Austin, R. Cammi, C. Pomelli, J. W. Ochterski, S. K. Morokuma, V. G. Zakrzewski, G. A. Voth, P. Salvador, J. J. Dannenberg, D. Dapprich, A. D. Daniels, Ö. Farkas, J. B. Foresman, J. V. Ortiz, J. Cioslowski and J. Fox, Gaussian 09 (revision B.1), Gaussian, Inc., Wallingford, CT, 2009.